8-2022

Stability analysis of ionically and electronically conductors in energy applications.

Tanner D. Whatley
University of Louisville

STABILITY ANALYSIS OF IONICALLY AND ELECTRONICALLY CONDUCTORS IN ENERGY APPLICATIONS

By

Tanner Whatley
B. S. Mechanical Engineering, Western Kentucky University, December 2020
M. S. Mechanical Engineering, University of Louisville, August 2022

A Thesis
Submitted to the Faculty of the
University of Louisville
J. B. Speed School of Engineering
as Partial Fulfillment of the Requirements
for the Professional Degree

Master of Science in Mechanical Engineering

Department of Mechanical Engineering
University of Louisville
Louisville, Kentucky

August 2022

STABILITY ANALYSIS OF IONICALLY AND ELECTRONICALLY CONDUCTORS IN ENERGY APPLICATIONS

By

Tanner Davis Whatley

A Thesis Approved On

July 29th, 2022

by the Following Thesis Committee

_____

Dr. Hui Wang, Thesis Director

_____

Dr. Thomas Berfield

_____

Dr. Noppadon Sathitsuksanoh

ACKNOWLEDGEMENTS

I would like to thank everyone that gave me encouragement and assistance in the process of completing the research for this thesis. I would like to thank specifically my parents and my closest friends that pushed me to always do my best, no matter how stressful things got during this time, to strive for the best possible outcome. I would also like to thank my coworkers and thesis director at University of Louisville, providing training and experience that I will take with me outside of the university and into my career. My coworkers progressing their education in PhD study gave me plenty of discussion describing their experience on similar experiments and provided help in any difficulties I had, to which I much appreciate. I would like to thank the University and Dr. Hui Wang personally for giving me the opportunity to participate in research and help in the pursuit of science advancement. Others to thank are my professors at WKU during my undergraduate studies that prepared and vouched for me to qualify for this kind of work for my graduate's degree. I would also like to thank Dr. Thomas Berfield and Dr. Noppadon Sathitsuksanoh for being members of the committee reviewing my research discussed in this thesis.

ABSTRACT

STABILITY ANALYSIS OF IONICALLY AND ELECTRONICALLY CONDUCTORS IN ENERGY APPLICATIONS

Tanner Davis Whatley

July 29th, 2022

The increasing need of electrical power around the world creates the search for sustainable energy to become a major stride in the manufacturing industry. The pursuit of energy storage systems being better, longer lasting, lighter, and cost effective have been a priority for companies, but one of the most crucial attributes in a battery should be its safety without the reduction in performance. For energy conversion and storage devices, such as solar cells and batteries, many important components are sensitive to air or moisture, therefore, the stability studies are important. This thesis focuses on two representative materials: hydrogenated carbon nanosheets (electrically conductive) and composite solid electrolytes (ionically conductive). The chemical structure, electrical conductivity, and water vapor transmission rate of hydrogenated carbon nanosheets have been studied to find the correlations between these properties with hydrogen content. For composite solid electrolytes, it has been studied the effect of compositions and synthetic parameters (humidity and temperatures) on their crystal structures and ionic conductivities. Study and recommendations towards solutions to improve stability are conducted and discussed.

TABLE OF CONTENTS

LIST OF TABLES

LIST OF FIGURES

Pages

I. INTRODUCTION

Over the past few decades, the growth of global warming has become quite noticeable, with the concern of burning fossil fuels, natural gas and other forms of energy consumption affecting the quality of life on Earth. The pursuit to minimize, if not irradicate, the use of these polluting fuels, has the change to renewable energy necessary for slowing the planet from increasing pollution and dangerous conditions for our future generations. With the increase in electrical consumption the process of converting virtually anything into energy has been in the process of study and improvement. The pursuit of hydropower, the Hoover Dam in Nevada for example, created in the early 1930s on the Colorado River, capable of producing enough power to serve 1.3 million people across Arizona, California, and Nevada.[5] The pursuit of wind power with multiple wind farms across the US with average wind turbine producing over 400,000 kWh per month, powering close to 450 homes each.[27] The pursuit of nuclear power which has been a controversial topic over many years due to the safety of a facility when a malfunction occurs, used by multiple countries power systems, with France having 70% of its power provided by nuclear reactors, Figure 1.[23]

The pursuit of solar power, with the number of home installations on their roofs continuously growing as the development of higher efficiencies and increased stability are under study and manufacturing. The ability and strive for energy have even led to decomposition of biodegradable materials such as trash in landfills, using the energy of

heat coming from the decomposing process to provide energy.[10] With many other forms of energy conversion, all these new and relatively old ways of converting existing energy into useable electrical energy is crucial to preventing the continuation of pollution to this planet.

Among various renewable energy resources, solar energy is abundant and environmentally friendly, thus it has immense potential to meet the rising energy demands. Photovoltaic devices that can convert solar energy into electric power are necessary for wider application of solar energy. In specific, organic-inorganic metal halide perovskite solar cells (PSCs), have gained great achievements since the first demonstration in 2009 and become the fastest growing photovoltaic technology. On the other hand, since solar energy has the feature of intermittent, time and location dependent, there is the necessity of power storage systems to achieve full potential of solar energy. Therefore, efficient energy storage systems such as batteries are required to ensure providing stable power supplies for various purpose electrical applications.

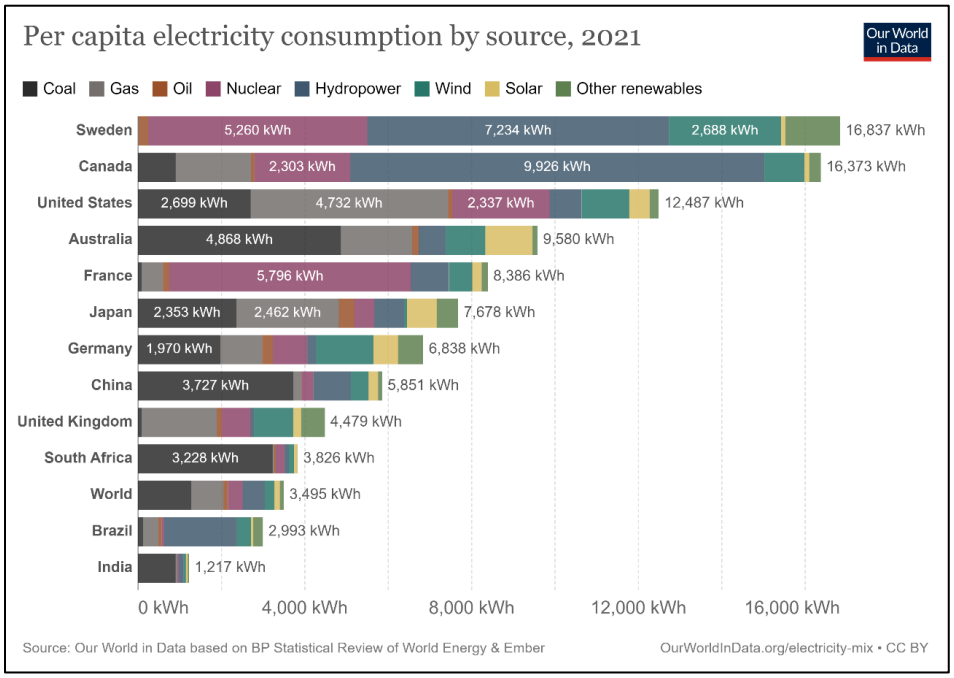

FIGURE 1 – Country's Categorized Electricity Consumption[23]

1.1 Perovskite Solar Cells

Even though the new sustainable energy converging systems are great for preventing pollution and substituting for the use of coal and natural gases, they are slowly improving with things like efficiency and stability. Efficiency is one of the main concerns for companies and consumers, making sure that they get the most energy as possible out of products. The other main concern for not only consumers but also engineers and scientists are the stability of these products, ensure that they are not only effective but also stable to last for long periods of time to produce that efficient energy and safe. Some energy converging and storage systems that have these issues are perovskite solar cells, PSCs, and batteries.

Perovskite is a material that produces solar energy conversion of about 19% for flexible and 25% efficiency for solid perovskite based solar cells in the past decade.[1] This has increased the interest in solar power for being useful on buildings and homes with the promise of higher efficiencies. A typical multilayered PSC contains five essential components: (1) a perovskite light absorber layer, (2) an electron transport layer (ETL), (3) a hole transport layer (HTL), (4) a transparent electrode and (5) a back electrode. As shown in Figure 2, the general working principle is when exposed to sunlight, photons are captured and electron-hole pairs are generated in perovskite layer; then electrons move to the ETL meanwhile holes flow towards the HTL, followed by the electrons and holes extracted to the transparent electrode and a back electrode, respectively. Later, the transparent electrode and back electrode are connected to form an external circuit. The

whole process is thermodynamically favorable when the valence and conduction band energy levels of the layers align.[36]

Perovskite materials face one main challenge of its stability in ambient environments, being exposed to oxygen and moisture causes deterioration, reducing the efficiency and eventually practically killing the cell in terms of being useful.[20] There have been studies on reducing the degradation of perovskite with the use of carbon coating. Acting as a hole transport layer to the solar cell components, the carbon prevents outside moisture from transferring through the cell, preventing moisture related reactions from happening.[1,3, 29] This creates a more stable environment for the inner workings of the cells, increasing shelf life of the most efficient solar cells in present history. The carbon-based layer in this new study has preserved the higher efficiencies of 15-18% over longer periods of time, over 1000 hours, whereas the degradation of PSCs previously would reduce from higher efficiencies starting at 20% but reducing much faster due to the lower stability.[8]

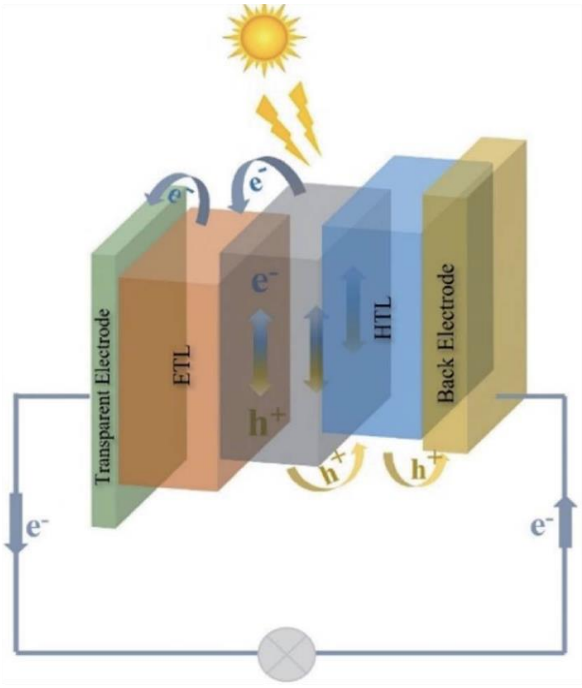

FIGURE 2 – Scheme of PSC Structure and Working Principles.[9]

1.2 Carbon materials to protect perovskite layer

Carbon nanomaterials such as graphene and carbon nanotubes are incorporated with polymers to form carbon–polymer nanocomposites. These materials have played different roles in PSCs, including as additives in the perovskite layer, electrodes, electron transporters, hole transporters, barrier layers, etc. The PSCs that contain carbon–polymer materials show enhanced performance including higher PCE values and long-term stability. In PSCs, the use of carbon materials as a protective coating on the perovskite surface is to prevent its degradation in working environment such as air and humidity. As shown in Figure 3, Ahn et al. designed a carbon-sandwiched PSC structure in which a lead halide perovskite layer was sandwiched by C60 and SWCNTs without metal electrodes.[2] The PSC devices with three HTMs (spiro-MeOTAD, PTAA and P3HT) incorporated in SWCNTs gave an average PCE of 17.0%, 15.3% and 13.6%, respectively. The supramolecular CNT–polymer hybrids were formed by inducing p–p interactions between polymers and CNTs; specifically, P3HT led to a much better stability than PTAA due to its planar conformation, which led to a close interaction with CNTs by wrapping around nanotubes.[9]

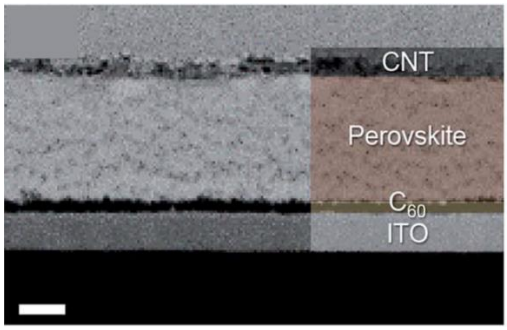

FUGURE 3 - SANDWICH structure of perovskite between two carbon layers for protection.[2]

1.3 Li-ion batteries and Solid-State Batteries

To take advantage of all these power systems, there is the necessity of power storage systems. Batteries have been around since the 1800s and have been the most important thing in today's day and age, being able to store power for everything from, phones, toys, power tools, technical equipment, remotes, vehicles, to laptops. The purpose of batteries allows the expansion of new power systems for less dependency on wall outlets and gas power; so that those tools can function anywhere to our most convenience. Batteries have been in development for over two hundred years, with many improvements that could be made such as capacity, cost effective materials, efficiency, stability and, an incredibly important criteria being safety of the user. Both dry and wet cells have issues involving the exposure of air or water, with the chemicals used in the batteries, fumes and combustion can occur when a powerful battery is damaged, and the exposed reactive components then are able to react to the outside environment.[19] These issues have noticed to be in the recent years with new development in technology such as electric cars and smart phones.

Batteries have three major components: anode, cathode, and an electrolyte, as seen in Figure 4. In the typical battery used for everyday devices, such as AA batteries, referred as a dry cell. The cells contain electrochemical materials that help transfer energy, with electrolytes that are a paste, reducing the need for water and any forms of liquid, hence the 'dry' cell. Another type of battery, commonly used in cars and other vehicles, referred to as a flooded or 'wet' cell. Like the name suggests, it is the exact opposite of a dry cell, needing liquid-based electrolytes used to help the process of transferring ions from the

anode to the cathode of the battery. Both kinds of cells are important in terms of convenience and level of capacity, with the dry cell being smaller, incredibly lighter whereas the wet cell is normally large, heavy, and larger in capacity; but the concern of safety is an issue with both as the increase in battery consumption becomes more apparent.

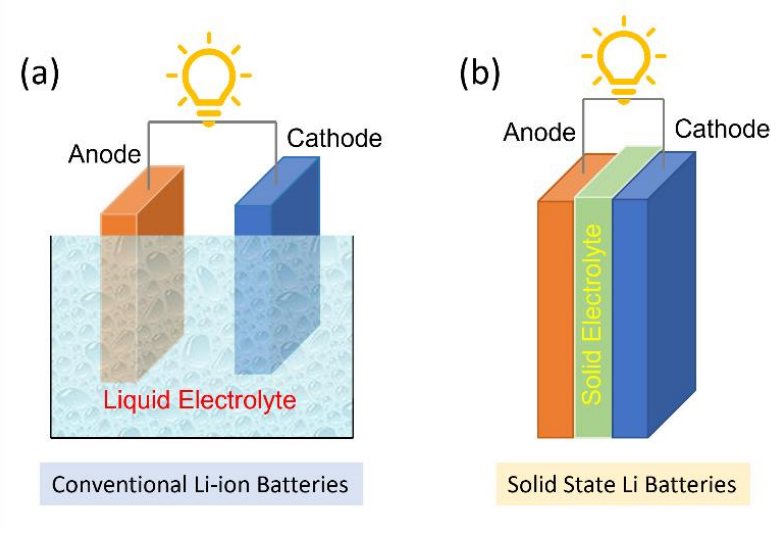

Figure 4 - Structure Schemes of (a) Conventional Li-ion Batteries and (b) Solid-State Batteries

There have been various kinds of materials studied in batteries to operate as an electrode and the main components of the battery's characteristics of Lithium and Sodium being the most promising.[33] Lithium is the most used due to its elemental characteristics and readability of it on Earth. Lithium-ion batteries are the most common battery used in today's market, for all forms of power storage, specifically for the rechargeable battery industry. Most recently the increase in electric vehicles (EVs) have created a higher demand for Lithium based batteries and the size of them to be quite large to hold enough energy to power the vehicles. Becoming the main component of a vehicle increases the necessity for safety with exposure to air and water being a must have for operating a

vehicle. This concern is under study as an incredible importance for the continuation and expansion of electric powered vehicles capitalized for everyday use. Being a major concern, the study and development of new components to improve the safety of the lithium-ion battery has increased in the past year with incredible progress in resolving the issue. The production capabilities are still yet to be determined, the manufacturing process of these components are far from obtained, with the process itself let alone the facilities to mass produce built for creating a safer future for battery and power storage systems. The issues that rise in this pursuit are finding the right components safe enough all while performing like the unsafe materials previously used. There has been in an increase in study on a promising solid electrolyte composite that is stable in the exposed atmosphere, being a capable candidate for safer lithium-ion batteries.

1.4 Argyrodite Solid State Electrolytes

The study of the Li-argyrodites has been conducted over the past few years due to the promising capabilities they show towards ionic conductivity through All-Solid-State-Lithium-Batteries (ASSLBs). Single or double doped argyrodites of sulfide-based materials have been suggested to achieve the higher conductivity in battery performance. Halogens such as Cl and Br have been the focus with their excellent performance reaching recorded conductivity of 10^{-2} – 10^{-3} S cm^{-1} with studies of Iodine doped argyrodites showing fewer promising results in the 10^{-7} S cm^{-1} range.[6] With multiple studies conducted for the Li_7PS_6 argyrodite (LPS) being doped as LPSX (X = Cl, Br, I) the chance of improving this electrolyte has been assessed for direct, pelletized studies with fewer in

composite polymer electrolyte membrane studies. As stated before, the biggest issue with electrolytes in lithium-ion batteries is the stability of them when exposed to the moisture and oxygen in the air, making the chance for ignition and combustion to be a possibility. Similar issues occur with active materials reacting and causing electrical complications such as shorting or creating a larger resistance reducing the performance of batteries and the testing results of the samples studied. A lot of the studies conducted for these various argyrodites have stated the use for inert gas chambers such as gloveboxes to fabricate these components for batteries due to their stability in atmospheric conditions. This will limit its capabilities in an industrial setting or will result in increase of expenses. On the bright side of these studies, there have been strides in preventing some of the issues, especially with the safety requirement. With the reaction of LPS and the moisture in the air, toxic gases are formed, which is why the use of polymers have been used to protect the argyrodite for the reactive material all while preserving some of the functional characteristics of the electrolyte.[14-15]

The use of doping the lithium argyrodite, LPS, with halogens allows for stability in atmospheric environments and increasing the conductivity. The capabilities of the halogen involved with the conductivity of the component in a battery is the production of halides and how they promote the HT phase.[34] This improves the conductivity by creating a subsystem environment for the electrolyte to create good ionic transfer between electrodes. Multiple accounts have shown the various attributes of the argyrodite and its doped variants. Techniques involving the lattice polarization of the electrolyte, monitoring the amount of halide anions, resulting lattice softness to have influence on the activation barrier and reducing the amount of energy necessary for ionic transport.[16] Variants involving

halogens such as Br, Cl, and I have studies showing Br and Cl showing the best performance. The use of another halogen, Fluorine, is a possible increase in performance of conductivity and a chance to provide a new electrolyte for manufacturers.[11] Due to the electron affinity of fluorine, it has the potential to provide enhancement in the electrolyte's performance in lithium-ion batteries. Other techniques have been on preserving the structure of the argyrodite by using different solvents and how they influence the electrolyte, preventing from further reaction between the active material in the drying process.[24] Even more so, the continuation of study on the electrolyte and its capabilities in a battery among the various doping's have provided much evidence in terms of characterization.

Using LPS electrolyte with polymer in a composite material, has shown to improve its stability in ambient environments. The use of polymer membrane fabrication process allows the stable interaction between the lithium and the electrolyte of the battery without producing an overabundance of Li dendrites, allowing for a more efficient and stable battery. With both LPS and the lithium salt being sensitive to oxygen and water but provide excellent performance, the use of protective polymer material is necessary to create something stable with promising performance. Even so, multiple variants have been previously studied in hopes to improve the performance, since the polymer is acting as a resistor in the product due to increased transfer distance and material characteristics.[4] More so towards the structure of the final product, with the timing needed to solidify the mixture, the reactions that take place between components are unwanted. Reactions that happen result in LiF, polysulfides, and Li_3PO_4.[25] This recently studied composite solid electrolyte containing LPS, has considerable characteristics in battery performance; achieving stable

cycling up to 1000 hours at a current density of 0.2 mA cm^{-2} and specific capacity of 160 mAh g^{-1} over 150 cycles.[26] This has made this promising candidate for a safer Lithium-ion battery.

1.5 Problem Statement and Thesis Overview

Due to the degradation of perovskite materials when exposed to water or high humidity, an encapsulation layer is added for protective purpose in PSCs. Thin carbon films have proven to protect perovskite materials from water/moisture and contribute to a stabile operation. Compared with pristine carbon, hydrogenated carbon nanosheets are expected to show better role in preventing water penetration due to the hydrophobic features. However, there is not sufficient studies on hydrogenated carbon nanosheets and its water vapor transmission rate and is suggested to be conducted.

Using sulfide-based composite solid electrolyte in solid-state batteries, the electrochemical and air stability has been greatly enhanced and reported. However, the composite preparation process has been mostly performed in either inert gas (protective) or dry and low humidity environments. Looking at the possible change in temperature and humidity, the stability analysis of the composite can conclude whether the ability to manufacture this form of electrolyte in high or moderate humidity (>40 RH%) is feasible. In addition, the parameters in drying process such as temperature can affect the reaction between components and the phase of the product drastically. Drying in a specific environment such as inert gas chambers like gloveboxes are useful for ensuring less reactions between outer system reactants, but for a mass production standpoint can be

incredibly expensive and probably not suitable for industrial purposes. With reactions involving the atmosphere and the active materials, the speed of fabrication should increase, and the humidity and other characteristics of the air should be monitored to optimize the quality of a process of mass production potential.

In this thesis, we have focused on two representative energy materials: hydrogenated carbon nanosheets (electrical conductors) and argyrodite-incorporated composite solid electrolytes (ionic conductors). The goal is to review and analyze the stability based on the results from the crystal and chemical structures, morphology, and conductivity.

After the introduction, the following section is an in-depth description of the instruments and equipment used in the process of the experiments, going into detail of what they are used for and why. The section after will go through hydrogenated carbon coating, which has shown potential in perovskite solar cell protection suggesting a possible protection to solid composite electrolyte as well. The next section will consist of the composite membrane electrolyte analysis conducted for humidity and temperature control to characterize structure and morphology. Both sections will be going in depth of observations and data collections. Each section will also discuss procedure for preparing samples and techniques of testing the characterization of each one. The section following will be the conclusion, making sure the results that were found have an explanation and clear understanding of what influence is described and desired through these experiments. Lastly the final section will be recommendations regarding what needs to be done to improve upon or further the research displayed in this thesis, ensuring the pursuit of an improved battery and solar cell can be achieved.

II. INSTRUMENTATION AND EQUIPMENT

There are several instruments and equipment that are described for material synthesis, sample preparation, and characterizations of the studied material throughout the paper. Illustration, description of function, and usage in these experiments are provided for each instrument in the following:

2.1 Hydrogenated Carbon Materials.

2.1.1 Preparation Instrument.

Tube Furnace. The hydrogenated carbon materials had been synthesized through a gas-solid reactions following the previous report.[9] Programed tube furnace (Thermo Scientific) had been used for the heat treatment (500 C) and dwell for different times (12 hour and 24 hours) The H content in the carbon materials had been controlled by the precursors.

FIGURE 5 – Tube Furnace

2.1.2. Characterization Instrument.

X-Ray Diffraction (XRD). The crystalline structure of the solid materials, including pristine argyrodite and solid composites with different compositions, have been examined using X-ray diffraction (Bruker D8 Discover). An XRD instrument works by the use of the diffraction of x-ray's sent by a laser, reflecting off the material, to a receiver. The angle that the ray shot is monitored along with the intensity of the reflection off the material. The stronger the intensity of the reflections are symbolized by peaks at the angles that x-rays were sent, which can later be identified to represent an element or compound through the comparison of a database of XRD readings. The XRD scanning was carried out in the range of 2θ=10~70 °C, and scanning rate of 1°C per min.

FIGURE 6 – X-Ray Diffraction Instrument (XRD)

Scanning electron microscope (SEM). The use of an SEM instrument, Scanning Electron Microscope, allows for the morphology of the material to be examined. The surface morphology of our prepared composite membranes was characterized by SEM. Being an electronic microscope the most important component to this is focusing of the sensors reading the material. The device involves a beam of electrons being sent to the surface of the material that are then reflected back. The electrons are scanned and scattered into a photo, showing the surface topography and composition of the sample. Depending on how atoms get excited by the electron beam, the intensity of the parts of the image can be detected and show a clear understanding of the surface being scanned. The specimen being scanned must be a certain size to fit in the container of the instrument, since the specimen is also placed under vacuum to prevent contamination and a proper environment for the electron beam to have clear readings. The images that can be captured are top surface, showing the topology of the piece or a side profile, capable of showing the internal

components of the specimen. With images and focusing being in the micrometers, the specimen does need to be small and placed carefully in the machine.

FIGURE 7 – Scanning Electron Microscope Instrument (SEM)

Four-probe instrument. The hydrogenated carbon materials were deposited on glass substrate and subjected to 4-prob device to measure the electrical resistance and conductivity. Sending DC current through 4 positions on the material, measuring the voltage change and calculates the level of resistance that it provides.

FIGURE 8 - 4Point-Probe for Electrical Conductivity Measurement

Water-vapor permeability. A water vapor permeability analyzer was used to examine the water vapor transmission rate (WVTR) for carbon materials on different substrates. The device uses a chamber of desiccants to pull moisture from a testing chamber that is holding the substrate. The moisture transfers through the substrate and the change of weight of the chamber is monitored and used to calculate the WVTR value over a period of time. The desiccant must be dried before conducting the tests making sure the humidity of the device drops below 10%, this allows for any vapor from the chamber to be pulled through the substrate and into the desiccant chamber.

FIGURE 9 – Water Permeability Analyzer

2.2 Solid Composite Electrolytes.

2.2.1 Preparation/Fabrication Equipment

Gloveboxes. The process to construct the solid composite electrolyte is a tedious and precise process but does not concern complex equipment to ensure a successful fabrication. However, the inorganic component in the composite is lithium argyrodite

(Li_6PS_5Cl or LPSCl), which is sulfide solid electrolyte and extremely sensitive to moisture and air. Therefore, the sulfide solid electrolyte is stored in the gloveboxes, which is filled with inert gas such as Argon (O_2 and H_2O<1ppm) to prevent any oxidization and eliminate any reaction with moisture from the outside environment.

FIGURE 10 - Glovebox

Hot Plate and Ultra-Sonicator. To prepare a homogeneous mixture from different components (inorganic, polymer, and Li salt) in the solvent, ultra-sonicator has been used. In addition, a hot plate has been used to promote the dissolving salt and polymer in the solution at elevated temperature.

FIGURE 11 – (LEFT) Hot Plate, (RIGHT) Ultra-Sonicator

Fume hood. With the mixing process complete, the mixtures have been poured in a petri dish, and rested in a fume hood to ensure a proper drying process. The air flow in the fume hood can be adjusted and controlled. In addition, a small box has been used to control the humidity environment in the fume hood. Inert gas flow has been employed to prevent the oxidation and reduce the humidity of box during the composite drying process.

With the few equipment and what they are meant to do for the process suggests a large-scale capability of simple mixing and drying at some form of humidity and temperature if the components are secure when mixing to prevent contamination in the compounds of the material.

FIGURE 12 – (LEFT) Chemical Vapor Hood, (RIGHT) Solid Polymer Electrolyte Drying Chamber

2.2.2 Characterization Equipment

The types of equipment that were used in the characterization of the material tested was to ensure that the material that was formulated had any reactions take place, the material was distributed properly, with correct structure or to determine the electrical capabilities of them in both individual and assembled battery configurations.

Electrochemical potentiostat. The electrochemical properties of the composite solid electrolytes, such as the ionic conductivity and battery cycling, had been examined using electrochemical potentiate (Bio-Logic VSP300). To evaluate the ionic conductivity, the electrochemical impedance spectroscopy was performed on the composite membranes. In addition, using the composite solid electrolytes, battery cycling had been performed under a certain current density.

FIGURE 13 – VP300, Potensiostat Device

III. HYDROGENERATED CARBON NANOSHEETS

In the case of batteries, high humidity environment is harmful for the preparation of high-quality composite solid electrolytes and destroy their crystal structures. Similarly, in Perovskite solar cells (PSC), the perovskite layer is also sensitive and unstable when exposed to high humidity, which significantly influence the performance of PSCs. Wu et al. reported that the resistance of perovskite microstrips can decrease by four orders of magnitude as increasing the relative humidity (RH) level from 10 to 95%, and the perovskite device lost photoresponsivity when the humidity above 85% RH level [ACS Appl. Mater. Interfaces 2019, Vol. 11, No. 33, pages 29821–29829].[2] To solve such instability issue, a protection film is considered to add on the top of perovskite layer to prevent the water penetration.

Among them, carbon materials such as graphene have been employed as the encapsulation layer for perovskite materials due to their excellent electrochemical and mechanical properties.[8] In comparison with pristine carbon, hydrogenated carbon materials that containing additional H-dopant show hydrophobic features, which may bring advantages to better inhibit water penetration and protect the perovskite layer.

In this work, we have studied the structural, elemental, and water vapor transmission rate (WVTR) as well as the electrically conductive property of hydrogenated carbon nanosheets that synthesized from solid-gas reaction.

3.1 Synthesis of Hydrogenated Carbon Nanosheets

The hydrogenated carbon nanosheets were synthesized by the reaction between lithium hydride (solid) and carbon monoxide (gas). The solid powder was then heated from room temperature to 500 ◦C at a rate of 10◦C /min and remained at the target temperature for 12 and 24 hours. After naturally cooling down, the samples were immersed in dilute hydrochloric acid solution and then washed with deionized water for several times until the PH of 7, finally dried at 80 ◦C for overnight. The hydrogenated carbon samples were provided by the collaborators at Wichita state university.

3.2 Structural, Morphology and WVTR Characterizations.

Structural and morphological characterizations. After synthesis, the obtained carbon materials were characterized for the phase identification by X-ray diffraction (XRD) by using Bruker D8 Discover in the range of 2θ=10-70◦. The Raman spectra were collected using a spectrometer between controlled wavelengths. The hydrogenated carbon nanosheets (500-12h and 500-24h) were subjected for FE-SEM to examine the surface morphology.

Elemental and electrical conductivity analysis. The elemental component of the carbon nanosheets were determined by a combustion elemental analysis method to detect the elements of C, H, N and O. The hydrogenated carbon coatings were deposited on non-conductive glass substrates. The thickness of carbon coatings was estimated around 10 µm. The electrical conductivity was examined by using a four-point probe instrument to measure the sheet resistance (Ohm/sq).

WVTR test. The hydrogenated carbon nanosheets were dispersed in isopropyl alcohol and deposited on two substrates (PET film and FTO-coated glass) by spray coating to form uniform coatings. These two substrates were selected due to being representative substrate for flexible- and flat-PSC devices, respectively. The thickness of carbon coatings can be controlled by the repeating times of spray deposition. The weight of carbon coating was also recorded by weighting the substrate before and after.

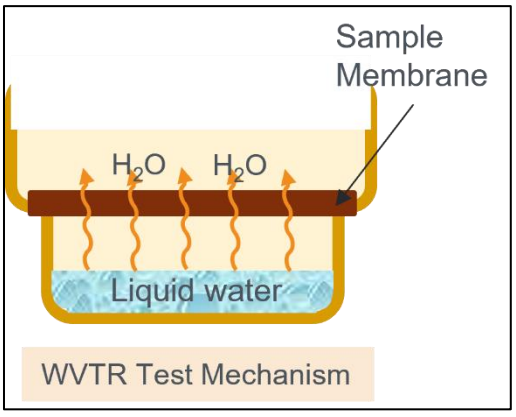

FIGURE 14. Test Mechanism

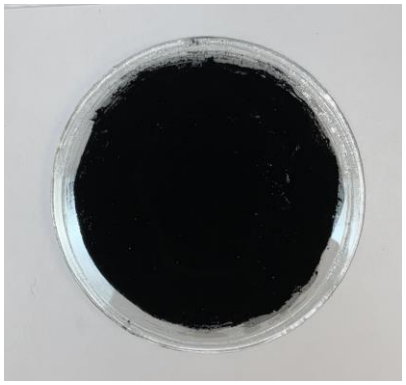

FIGURE 15 - Carbon Coated Substrate

3.3 Results and Discussion.

3.3.1 Elemental and Morphology Analysis of Hydrogenated Carbon Nanosheets

The synthesized carbon nanosheets were subjected for elemental analysis to characterize the hydrogen contents by examining the C, H, elements by combustion and O contents by pyrolysis. After heating treatment at 500 ◦C, both carbon nanosheets (500-12h and 500-24h) contain three elements of carbon, hydrogen, and oxygen. When the heating time increases from 12 hours to 24 hours, the C content increases from 80.62% to 85.14% in the carbon nanosheets while the H content decreases from 1.93% to 1.19% as seen in Table 1. In comparison, the commercial active carbon only shows the H content of 0.39%, which is much lower value than that of hydrogenated carbon nanosheets. SEM images in Figure 16 show the surface morphology of 500-12h and 500-24h samples, both show thin and curved nanosheets.

TABLE 1. ELEMENTAL ANALYSIS OF CARBON NANOSHEETS.

Samples	Elemental analysis			
	Carbon (%)	Hydrogen (%)	Oxygen (%)	Nitrogen (%)
500-12h	80.62	1.93	17.40	<0.05
500-24h	85.14	1.19	10.06	<0.05
Active Carbon	68.75	0.39	25.65	5.21

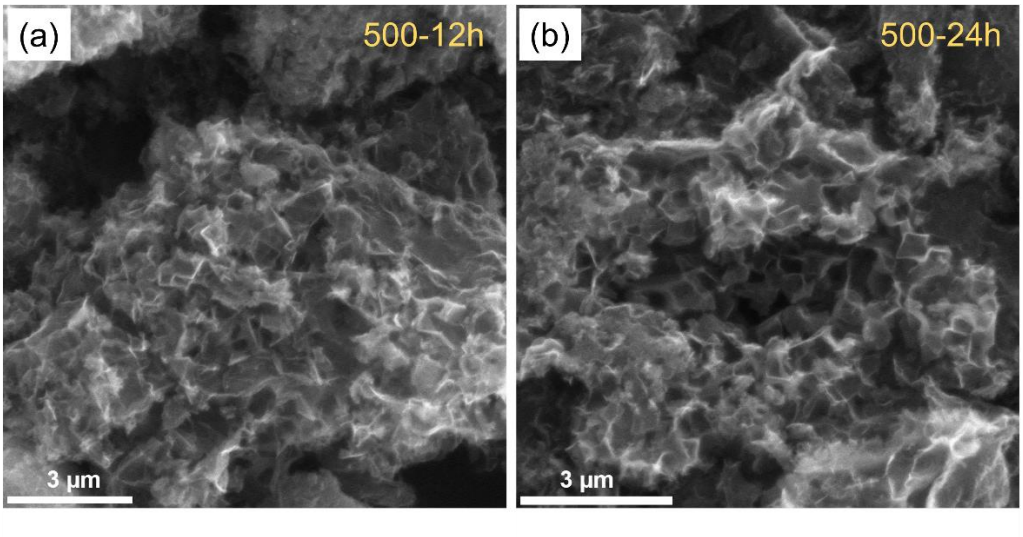

FIGURE 16. SEM Images of Carbon Nanosheets.

3.3.2 Structural Characterization of Hydrogenated Carbon

For hydrogenated carbon nanosheets, XRD characterization is employed to examine the structure information. As shown in Figure 17, both samples (500-12h and 500-24h) display the characteristic diffraction peak at $2\theta=24.8^{o}$, corresponding to (002) plane. There are no other impurity peaks in the XRD patterns. In addition, the synthesized carbon nanosheets show broad peak instead of the sharp diffraction peaks for graphite, which suggests the fine size of nanosheets. In addition, the Raman spectroscopy is employed to

further understand the structure in hydrogenated carbon nanosheets. Figure 18 presents the Raman spectrum of 500-12h sample, which clearly shows the D band at ~1300 cm-1 and G band at 1550 cm-1. The D band and G band are corresponding to the vibrations of SP3 hybrid and SP2 hybrid, respectively. The D band in 500-12h sample has comparable intensity with that of G band, reflecting its disordered structure.

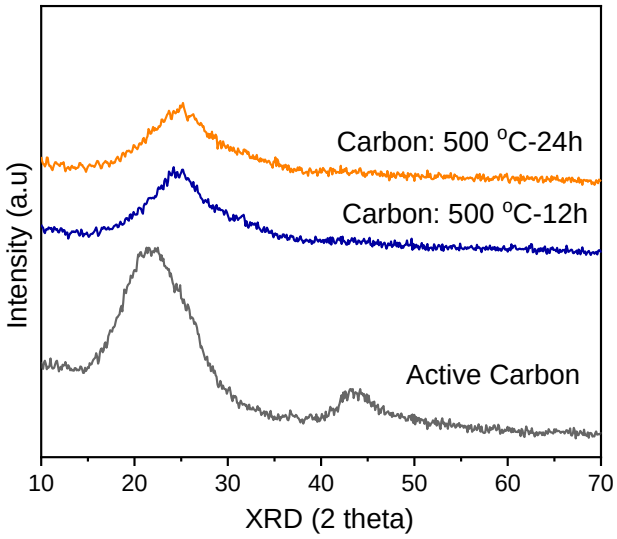

FIGURE 17. XRD Patterns of Carbon Nanosheets: 500-12H, 500-24H and Active Carbon.

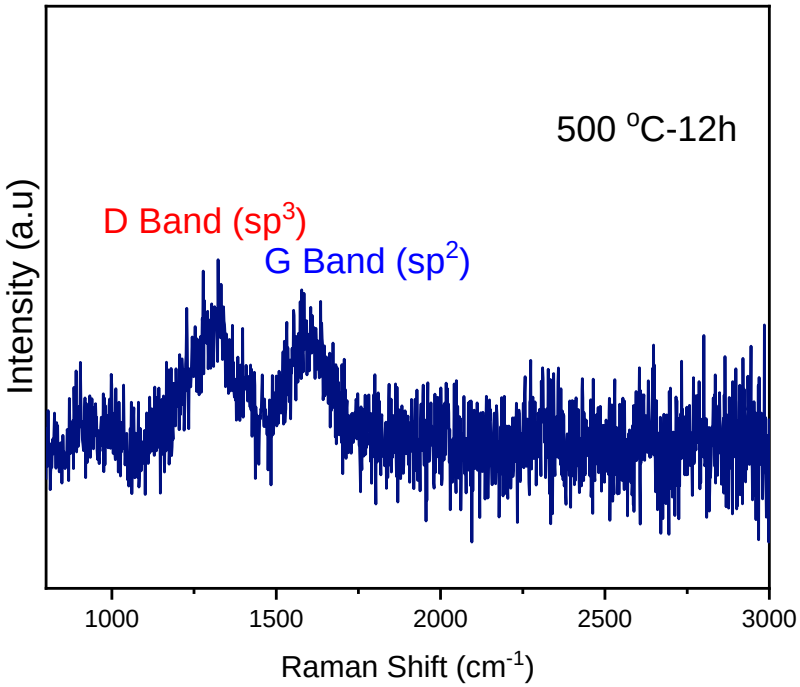

FIGURE 18. RAMAN Spectra of Carbon Nanosheets Obtained at 500C for 12H.

3.3.3 Water Vapor Transmission Rate Test of Hydrogenated Carbon Nanosheets

Using PET film (~140 μm) as substrates, hydrogenated carbon nanosheets samples (500-12h, 500-24h) were deposited to form thin carbon coatings. The WVTR value of bare PET film is about 3.3 $\times 10^{-4}$ g/cm^2/day. Figure 18 shows the WVTR variation trend of carbon coatings on PET substrates as increasing the weight of carbon per area. With the same amount of carbon (0.4 mg/cm^2), the WVTR values of 500-24h and 500-12h samples are about 1.4×10^{-4} g/cm^2/day and 1.1×10^{-4} g/cm^2/day, respectively, both of which are much lower than that of active carbon (~3×10^{-4} g/cm^2/day). In addition, if compared with bare PET substrate, the synthesized carbon nanosheets 500-24h decreases the WVTR rate by

58%, and the sample of 500-12h reduce the WVTR value by 62%, respectively. Both samples are better than the water penetration prevention of active carbon, which only decrease by 10% than bare PET.

It is observed that the 500-12h sample carbon nanosheets has lower WVTR values than those of 500-24h sample. The decreased water penetration rate is considered with the H-content in the carbon nanosheet. Moreover, it is observed that the higher H-content leads to a lower value of WVTR, which explains that the lower water penetration rate in 500-12h sample (1.95% H) than 500-24h sample (1.15% H).

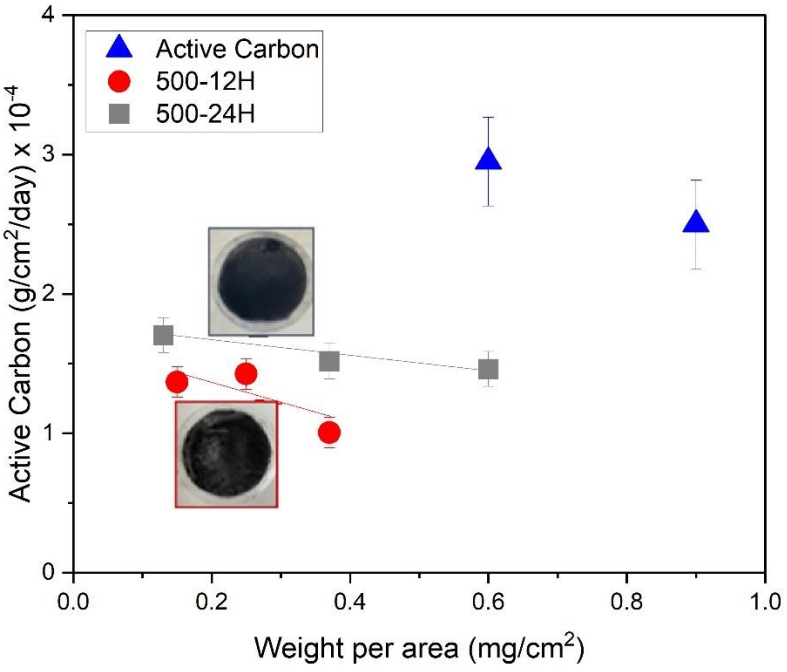

FIGURE 19 - PET Film WVTR Analysis on PET Film

Other than PET film, FTO coated glass is also popular substrate for PSC devices. Following similar procedures, hydrogenated carbon nanosheets were deposited on FTO

glass substrates to form homogeneous films (~15 µm). Figure 20 illustrates the comparison of the coated samples to the base. The FTO-coated glass exhibits a WVTR value of 3.4×10^{-6} g/cm^2/day, which is two orders lower than that of PET substrate. After coating carbon nanosheets, the 500-24h sample on glass decrease the WVTR value to 1.6×10^{-6} g/cm^2/day and 500-12h sample leads to a lower value at 1.2×10^{-6} g/cm^2/day. This observation is similar with carbon nanosheets coatings on PET substrate, where the 500-12h sample with higher H-content results in lower WVTR value than that of sample with lower H-content.

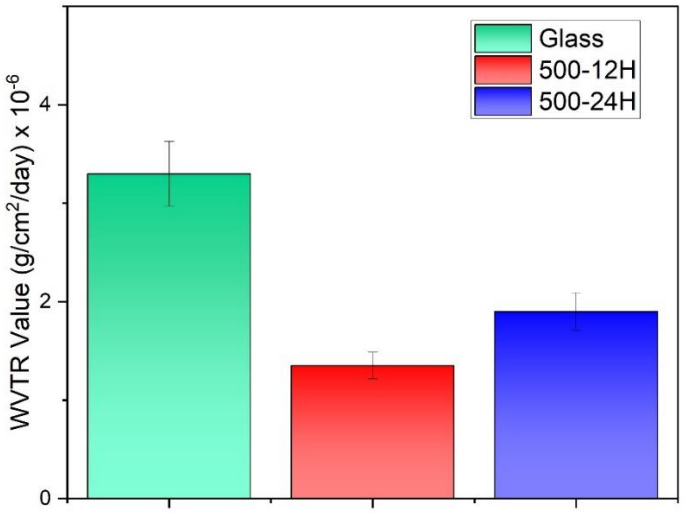

FIGURE 20 - Carbon Coated Glass Comparison to Base WVTR Values

3.3.4 Electrical Properties of Hydrogenated Carbon Nanosheets

The sheet resistance of hydrogenated carbon nanosheets was measured to examine their electrical conductivity. Each sample was measured for four times. As seen in Table 2 The 500-12h carbon nanosheets sample exhibits the sheet resistance of 91.3 Ω/sq while the 500-24h sample shows lower sheet resistance of 45.4 Ω/sq, suggesting higher conductivity

for the sample after longer heating treatment time. The improved electrical conductivity for 500-24h sample is due to higher C-content and low H-content.

TABLE 2. THE ELECTRICAL CONDUCTIVITY OF CARBON NANOSHEETS

Samples	Sheet Resistance (ohm/sq)				
	Test 1	Test 2	Test 3	Test 4	Average
500-12h	87.6	89.2	92.9	95.5	91.3
500-24h	39.4	48.7	49.8	43.5	45.4

In summary, hydrogenated carbon nanosheets were synthesized and studied on their elemental, structure, and morphology as well as electrical conductivity. In addition, the water vapor transmission rate of the hydrogenated carbon nanosheets was also examined and correlated with H-contents. It is demonstrated the positive affect of the hydrogenated carbon nanosheets on reducing the WVTR values, in which higher H-doping content in carbon nanosheets results in lower WVTR value. Due to such low water penetration rate, the hydrogenated carbon nanosheets may provide higher protection to moisture sensitivity materials such as perovskite in PSCs, and thus increase the stability of PSC performance in practical applications with high humidity.

IV. COMPOSITE SOLID ELECTROLYTES

In solid-state batteries, composite solid electrolyte plays an important role to separate the electrodes and transport ions between the anode and the cathode, resulting in electrical power that can be used in an electrical circuit. The process studied previously is a cost-effective way of producing solid composite electrolyte to be used for components of solid-state Li metal batteries. When in preparation, there are technical monitoring that is expected: humidity, temperature, quantity, and timing that are crucial conditions that mark to a successful fabrication process. These experiments were successful in the process of synthesizing useful electrolytes that demonstrate functioning battery cycles. This chapter summarizes the main results on studies of composite solid electrolytes discussing characterization and performance in battery assembly.

4.1 Synthesis of Composite Membranes with Different Compositions

4.1.1 Synthesis of Li_6PS_5Cl argyrodite.

For the argyrodite Li_7PS_6, LPS, there are many variants on doping, such as Br, I, and Cl with Cl and Br being the most promising in performance. As described in previous report, the synthesis of the non-doped LPS is through a mixture of Li_2S and β-Li_3PS_4, dissolved in ethanol in an argon filled glovebox.[25] The mixture then heated to 90 °C under vacuum for no longer than an hour to evaporate the solvent yielding a white precipitate and

then treated at 200 °C for 1 h to obtain the final product of LPS.[32] For preparing the Cl-doped LPS (Li_6PS_5Cl), a sociochemical ratio of LiCl had been added into the mixture of Li_2S and β-Li_3PS_4 in ethanol solution, following by the same heating treatment to produce Li_6PS_5Cl argyrodite, LPSCl.

4.1.2 Synthesis of Li_6PS_5Cl incorporated composite solid electrolyte

The composite solid electrolyte consists of inorganic argyrodite Li_6PS_5Cl (LPSCl), polyvinylidene difluoride (PVDF-HFP) polymer, and Li salt (LiTFSI). First, LPSCl powder, polymer powder, and Li salt were dispersed/dissolved in tetrahydrofuran (THF) solvent, respectively. The PVDF-HFP used in the experiments were pellet shaped, which requires a relatively longer dissolving process to form a translucent liquid solution. The concentration of solid powders in solvent is about 0.1g/mL. Second, these three components were mixed together and carried out ultrasonic treatment/stirring at room temperature to obtain homogeneous mixtures, which is important for uniform composite membranes. Later, the mixtures were poured on clean petri dishes and drying for 4 hours at room temperature to produce the final composite solid electrolyte membranes. The obtained composite solid electrolyte membranes are flexible and have thickness around 180± 20 μm (Figure 21).

FIGURE 21 – Solid Composite Membrane Example

During the preparation process for the composite solid electrolytes, two factors have been controlled: (1) the contents of inorganic component (LPSCl); and (2) the humidity in drying conditions. First, the contents of inorganic component (LPSCl) had been varied by changing the weight of powder before mixing the solution. Various batches of solid composites that contain large range concentrations of LPSCl were prepared, which including 5 wt%, 10wt%, 15 wt%, 20wt%, and 30wt%. Second, different drying environments include ambient environment with high humidity (50-70%RH); low humidity environment (30-40%RH). For the composite membrane preparation, the homogeneous mixture is significant to obtain a uniform membrane. Or else, aggregation of particles in the membrane is observed (Figure 22).

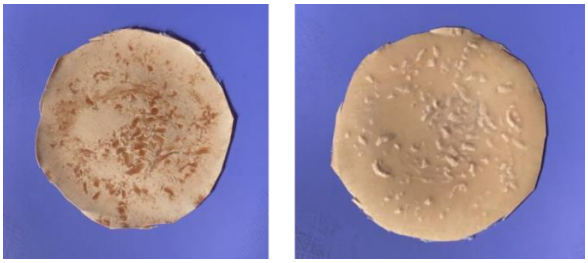

FIGURE 22- Examples of Inhomogeneous Composite Membranes.

4.2 Characterization of the Samples

4.2.1 Structural characterizations.

XRD characterizations were performed to identify the crystalline structures of prepared composite solid electrolytes. The composite membrane was put on zero-background glass substrate, which were loaded on sample stage of the XRD instrument without any further protection. For all samples, their XRD patterns were collected between 2θ=10-70 degrees with scanning rate of 0.05° per second. Once the tests are conducted and the data has been consolidated into a clear graph, a material science database could then be used to look up any compounds, elements, or reactants involved in the mixture to compare XRD peaks of intensity and having matching peaks can confirm the contents of the sample.

4.2.2 Morphology Characterization of the Prepared Samples

For conducting examinations of the sample in terms of morphology, SEM characterization was carried out to get an incredibly close image of the samples. The SEM tests allows to determine whether the surface is homogeneous or not. The ideal composite sample should include a well distributed and uniform material, being crucial for a good performance in a battery, allowing for good contact and efficient ion transport between the electrodes.

4.2.3 Electrochemical Characterization of the Prepared Samples.

Ionic Conductivity Test. For ionic conductivity measurements, the cutting of the membrane into a small circle using a hole punch, roughly ½ inch diameter. The composite membranes were sandwiched between two pieces of stainless-steel (blocking electrode), which were loaded in coin cells and pressurized by a press to secure the electrolyte between the stainless-steels and provide a better surface connection between the coins and the electrolyte to accurately monitor the impedance. Electrochemical impedance spectra (EIS) were measured and collected at room temperature to calculate the ionic conductivity following the equation of $\sigma = \frac{L}{A \times R}$, where σ is ionic conductivity (S cm^{-1}), L is thickness of membrane samples, A is the cross area of membranes, R is the resistance from Nyquist plot.

Battery Assembly and Cycling. The assembled batteries in coin cells have structure as shown in Figure 23. The batteries have composite membrane (containing 20 wt% LPSCl) as solid electrolyte; Li metal as the anode, and LiFePO4 as the active cathode. As the anode, thin Li foils have thickness of 150 μm. The composite cathode has LFP: PVDF: carbon black with weight ratio of 8:1:1. Small amounts of liquid PC/LiTFSI was added between the composite solid electrolyte and electrode to reduce the resistance at the solid/solid interfaces.

The battery is assembled in a glovebox to preserve the lithium foil and components. The battery is then taken out of the glovebox and placed in a hydraulic press to apply pressure to seal and provide surface contact between the electrodes and the electrolyte, being careful not to apply too much pressure to damage the casing or crush the components

into shortening. The battery is tested for voltage with a voltmeter and then is placed on the Bio-Logic device to run through cycles of charging and discharging and recording up to 100 cycles to show the quality of the performance.

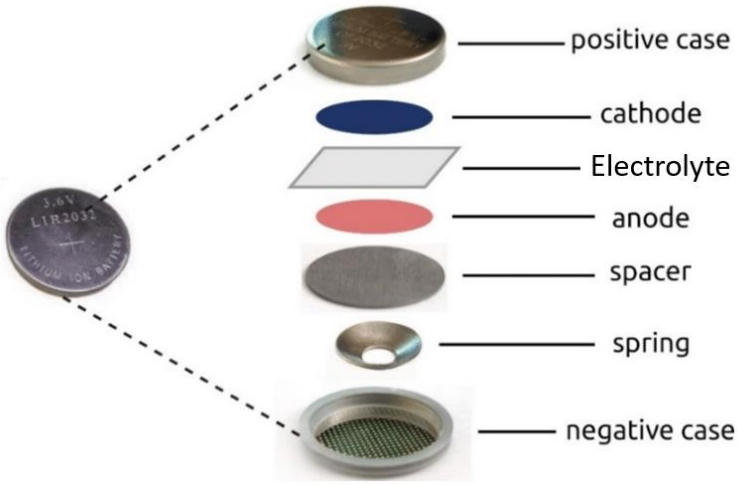

FIGURE 23 – Battery Assembly Diagram

4.3. Results and Discussions

4.3.1 Composite Solid Electrolytes Membranes with Various Contents of Argyrodites

The composite solid electrolytes consist of three components: LPSCl inorganic sulfide, PVDF-HFP, and LiTFSI salt. To understand the influence the contents of argyrodite sulfide on crystalline structures, we had prepared composite solid electrolyte membranes that containing four different weight ratios of LPSCl sulfide: 10 wt%, 15 wt%, 20 wt%, and 30 wt%. The prepared composite solid electrolytes were subjected for XRD characterizations for the crystalline structures.

Figure 24 shows the XRD patterns of composite electrolytes that contain 10 wt%, 15 wt%, 20 wt%, and 30 wt%, in compared with pure LPSCl argyrodite (100 wt%), and

pure polymer electrolyte (0 wt% sulfide). For the polymer membrane without any inorganic component, there are two broad bumps at 2θ=20°, 40° that come from the polymer (PVDF-HFP) and Li salt. After adding 10 wt% LPSCl sulfide argyrodite, those two broad peaks are still dominant although three new diffraction peaks at 2θ=43˚, 45˚, and 50˚ appear. When the LPSCl content increases to 15 wt%, new strong diffraction peaks at 2θ=14° and 36.5° (strongest) appear, which are much stronger that those bumps from polymer electrolyte. With the highest content (30 wt%), the composite solid electrolyte exhibits complexed diffraction patterns with the strongest peaks at 2θ=14°, 33˚, and 34°. These strong diffraction peaks are not matched with the characteristic peaks of LPSCl argyrodite sulfide at 2θ=14°, 30.5˚, and 31.2°. Since the preparation of composite solid electrolyte happening in ambient environment without inert gas protection, the mismatch is considered due to the possible reaction between sulfide with moisture in humid air.

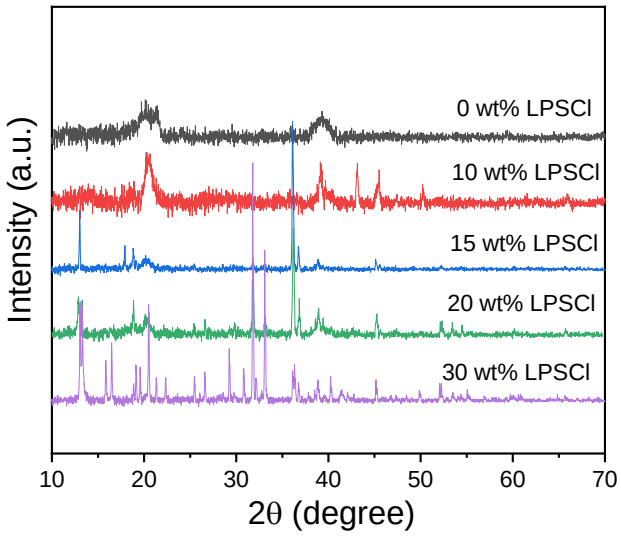

FIGURE 24 – XRD Results of Weight Percentage Differences of LPSFCL Membrane

For comparison, we also prepared the composite electrolyte with 20 wt% LPSCl and dried the membrane inside glovebox that filled in Ar gas with low humidity and oxygen (O_2, H_2O < 1ppm). Figure 25 shows the XRD patterns for the 20 wt% LPSCl-composite electrolyte that prepared in glovebox, which clearly display characteristic diffraction peaks at 2θ=25˚, 30˚, 31° that indexed to argyrodite structure. This result suggests that the argyrodite structure is well remained in the composite solid electrolyte if the preparation process is under inert gas protection and low humidity, which further confirms that the humidity strongly influence the synthesis process of composite solid electrolytes with LPSCl as the inorganic component. EIS measurements were performed on the composite solid electrolyte membranes that contain different weight ratios of LPSCl argyrodite sulfide to evaluate the composition dependence of ionic conductivity. The lowest ionic conductivity is observed for the 15 wt% LPSCl composites while the highest value for the 30 wt% composite.

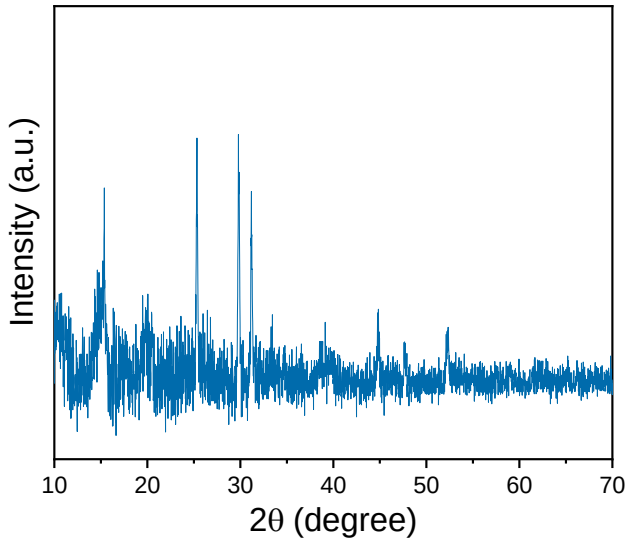

FIGURE 25 – XRD Results of LPSFCL Composite Membranes Prepared in Glovebox

4.3.2 Influence of Humidity on the Structure of Composite Membranes

The point of measuring the level of humidity and temperature is for finding the fastest and most effective way of producing this solid electrolyte, which enables for low-cost manufacturing process. In the composite solid electrolyte, sulfide argyrodite is the most moisture-sensitive, therefore, high sulfide content at 30 wt% LPSCl is selected to study the effect of humidity on structure of composite membranes. Following the same dispersion/dissolving and mixing steps, the homogenous mixtures were casting in petri dishes and dried under four different humidity levels (40, 50, 60, 70%RH), respectively. The obtained composite solid electrolyte membranes were characterized by XRD for the crystal structures.

Figure 26 displays the XRD patterns of composite solid electrolyte membranes that dried under 40%, 50%, 60%, and 70% relative humidity, which show tremendous variation of diffraction patterns as increasing the humidity levels. With 30 wt% LPSCl in the composite solid electrolytes, even though under the humidity of 40% RH, there is very minimal traces of characteristic diffraction peaks for LPSCl (2θ=26˚, 29˚, and 31°). Instead, the composite sample after 40 RH% show strong diffraction peaks at 2θ=21˚, 32˚, and 34°. This observation indicates that the PVDF-HFP polymer may not be able to fully protect high concentration of LPSCl sulfide at 30 wt% from the exposure to air and moisture in the composite when drying in an open environment. Interestingly, as increasing the humidity level during synthesis process, these strong diffraction peaks become to disappear, and new peaks at 2θ=36˚, 38° appear and become stronger. At the highest humidity level of 70% RH, the peak at 2θ=36˚ is the dominate one, along with other minor

peaks. The outcome would then be compared to experiments conducted in a glovebox to show the quality of the compounds under extremely low levels of humidity (H_2O< 1ppm). The glovebox trials were performed following the same procedures to ensure the humidity and oxygen exposure were the only varying conditions.

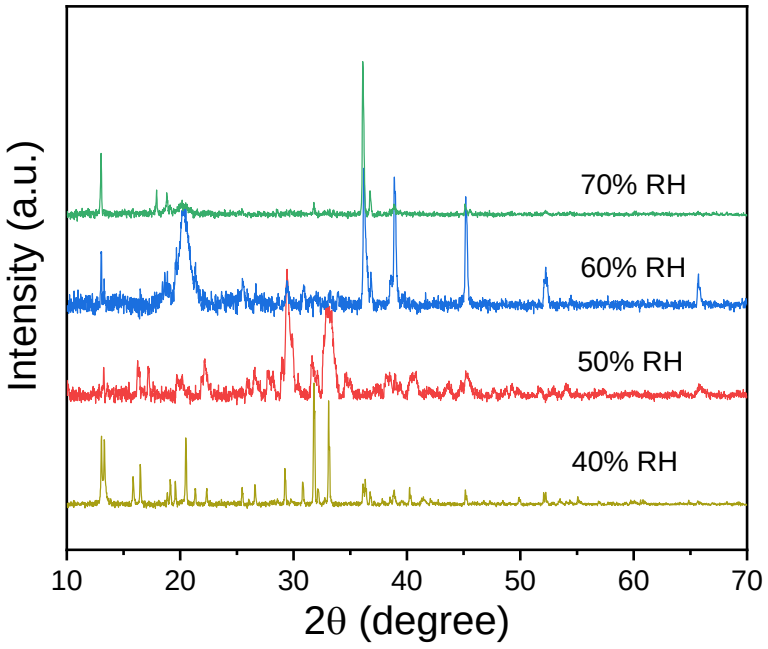

FIGURE 26 – XRD Results of Humidity Monitoring of LPSFCL Composite Membranes

The composite sample (20 wt% LPSCl and 40% RH) was examined on its ionic conductivity, which shows the value of 1.05×10^{-3} S cm^{-1} at room temperature. For the impedance measurements, the composite membrane is sandwiched between two stainless steel pieces (as block electrode). Figure 27 shows the Nyquist plots of EIS measurement for this sample under different temperatures, all of which have a spike at the low frequency. The resistance continues to decrease as increasing temperatures from 20 to 70 °C, suggesting the increase of ionic conductivity at higher temperatures. The Nyquist Plot also

gives viable information for determining the level of impedance for each temperature, allowing for the illustration of an Arrhenius plot to be made and calculate the activation energy as seen in Figure 28. Activation energy was determined to be 0.193 eV/mol suggesting lower activation energy associated with high conductivity.[4]

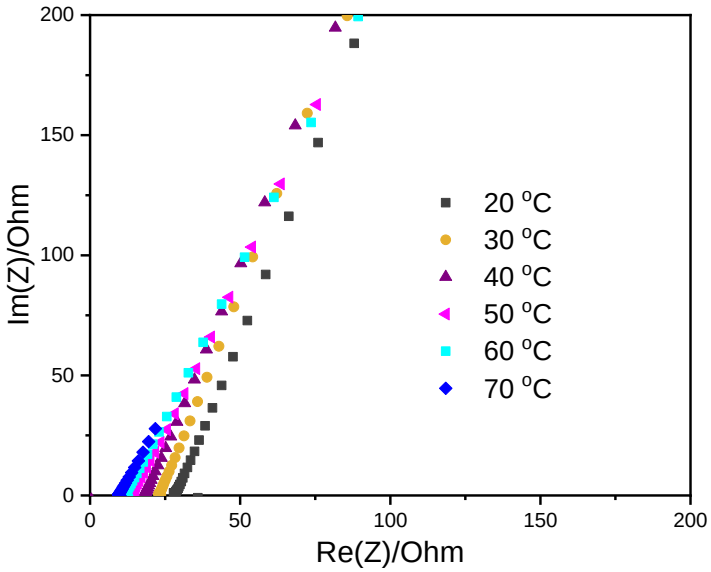

FIGURE 27 – Nyquist Plots of EIS Measurement for Sample Under Different Temperatures

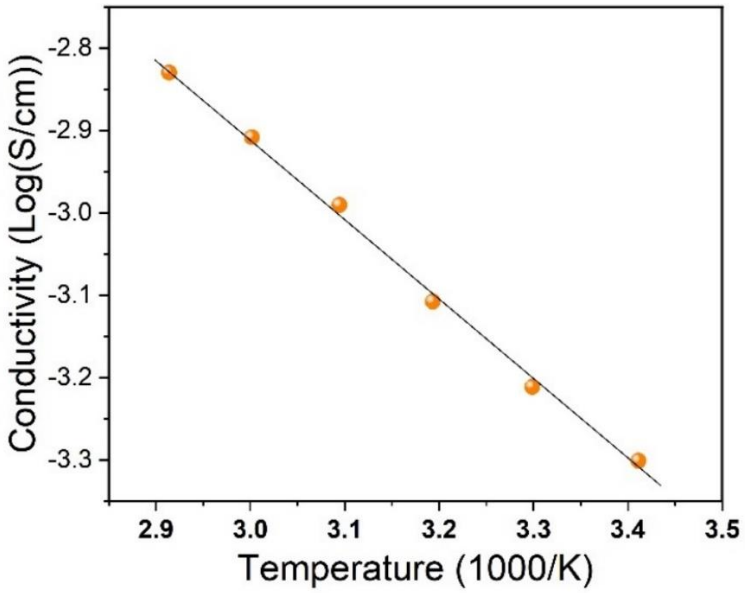

FIGURE 28 – Arrhenius Plot of LPSCl Composite Membrane

4.3.3 Influence of Drying Temperature on the Structure of Composite Membranes

During the drying process, the hot plate can be used to raise temperatures, which facilitates the solvent evaporation and reduces the required time to obtain the final composite solid electrolytes. Although the shorter drying duration can improve the product efficiency for industrial production, the THF as polar solvent may cause side reactions with argyrodite sulfide at elevated temperatures. Therefore, composite solid electrolytes with the same sulfide content (20 wt%) were prepared following the same procedures of mixing and stirring but dried under three different temperatures of 40 °C, 50 °C and 60 °C, respectively. When the drying temperature increases, the color of composite membranes changes from light yellow, to yellowish and dark yellow (Figure 29).

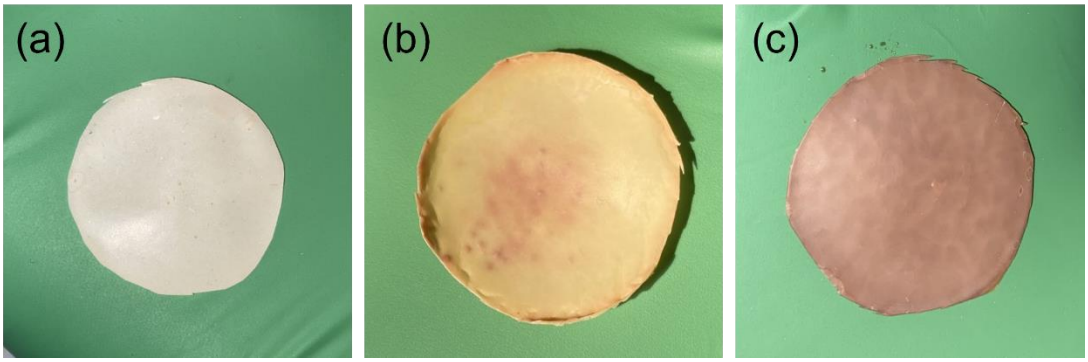

FIGURE 29 – Coloration Change of Composite Membranes of Various Temperatures (a) 40 ºC, (b) 50 ºC, (c) 60 ºC

Figure 30 shows the XRD patterns of 20 wt% LPSCl incorporated composite solid electrolytes that prepared after different temperatures. For the composite sample after 40°C, strong diffraction patterns are observed with highest peaks of 2θ=32˚, 36°, while these peaks are not ascribed to LPSCl. However, at higher temperatures of 50 and 60 °C, these diffraction peaks dramatically decrease and disappear ultimately. When the drying temperature at 60 °C, only two broad peaks at 2θ=20.1˚ and 40.2˚ are remained, which come from the polymer electrolyte. This observation suggests that the crystalline structure of sulfide had been disappeared at higher drying temperatures. Also, it is confirmed through XRD observations that the temperature has influence of the structure of the membrane.

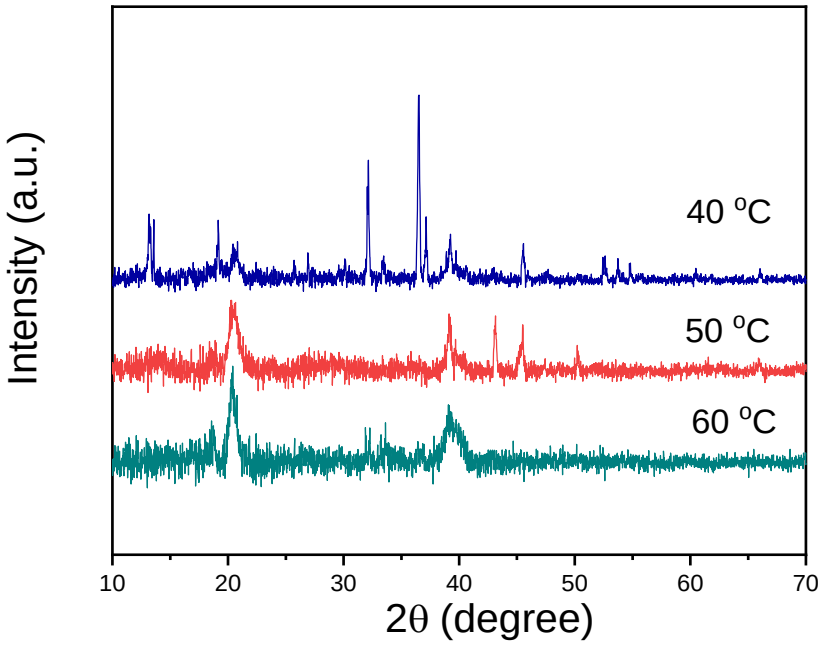

FIGURE 30 – XRD Results of Temperature Analysis of LPSFCL Composite Membranes

Beside the structure, we also measured the ionic conductivities of composite electrolytes (20 wt% LPSCl) after dried after different temperatures (40, 50, 60 °C). The Nyquist plots of these composite membranes are shown in Figure 31, which show the impedance increase trend for increasing temperatures from 40 to 60 °C. The sample after 40 °C exhibits the highest ionic conductivity of 1.02×10^{-3} S cm^{-1} at room temperature, followed by the sample after dried at 50 °C at 0.77×10^{-3} S cm^{-1}, and the composite membrane dried at 60 °C with the conductivity value of 0.23×10^{-3} S cm^{-1}.

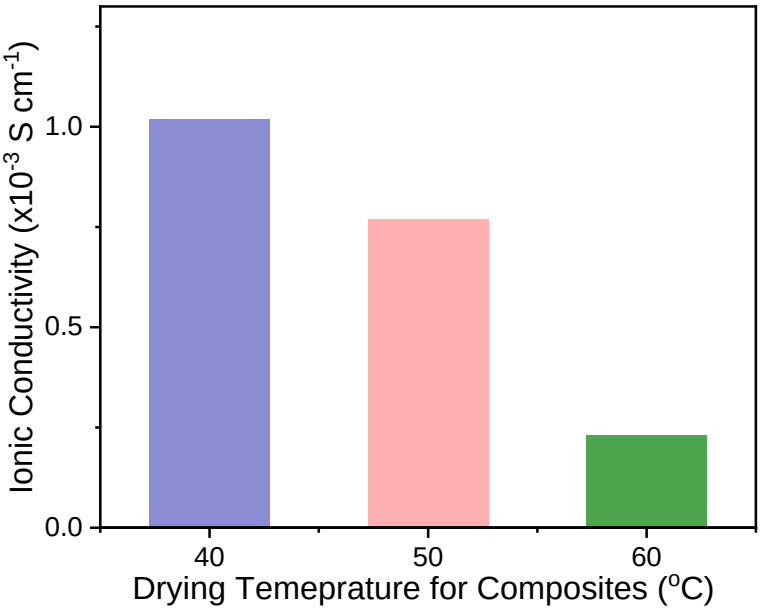

FIGURE 31 – Ionic Conductivity of Composite Samples After Drying Various Temperatures.

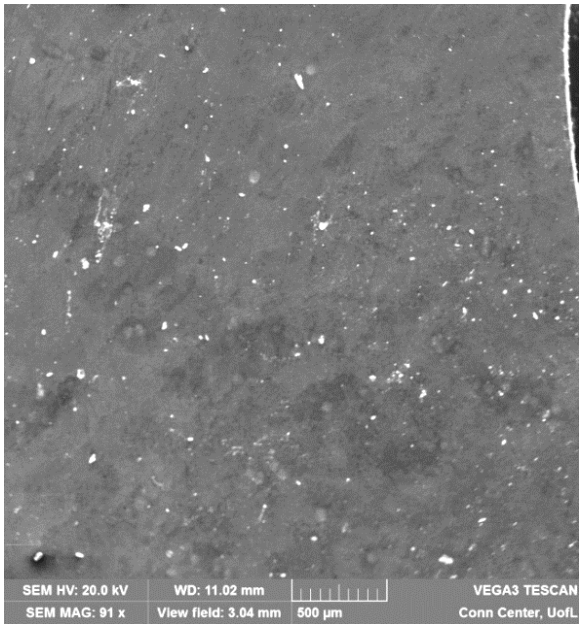

FIGURE 32 – SEM Scan of Composite Membrane

4.3.4 Battery Performance

The composite solid electrolyte membranes that are prepared under moderate humidity environment had been employed to assemble batteries by using Li metal as the anode, LFP as the cathode with theoretical specific capacity of 170 mAh g^{-1}. In the composite cathode, it has the active material (LFP), carbon and binder with weight ratio of 8:1:1. Small amount of PC/LiTFSI was added at interface to reduce the solid/solid contact resistance. The assembled batteries were cycled under a C-rate of 0.1 C with the voltage window of 2.5-4.0 V.

Figure 31 shows the specific capacity and efficiency curves of composite solid electrolyte-based batteries. The initial capacity of this type of battery exhibits 120 mAh g^{-1}, which slightly increases to 138 mAh g^{-1} in the 2^{nd} and 3^{rd} cycles. The high capacity remains well until to 8-9 cycles, but beyond it, the capacity suddenly drops to ~90 mAh g^{-1} after 10^{th} cycles and the slightly to 70 mAh g^{-1} after 20^{th} cycles. Nevertheless, there is the capacity increase happening between 20-30^{th} cycles, after that the battery capacity goes back to 65-79 mAh g^{-1}. During the charge-discharge periods, the coulombic efficiency for the 1^{st} cycle is about 92% due to the formation of a solid electrolyte interphase (SEI) layer, and then remains above 98.5% for the rest of cycles. Although the low capacity happens after 50^{th} cycles, this battery is keep running for 1000 cycles without short, suggesting its electrochemical stability.

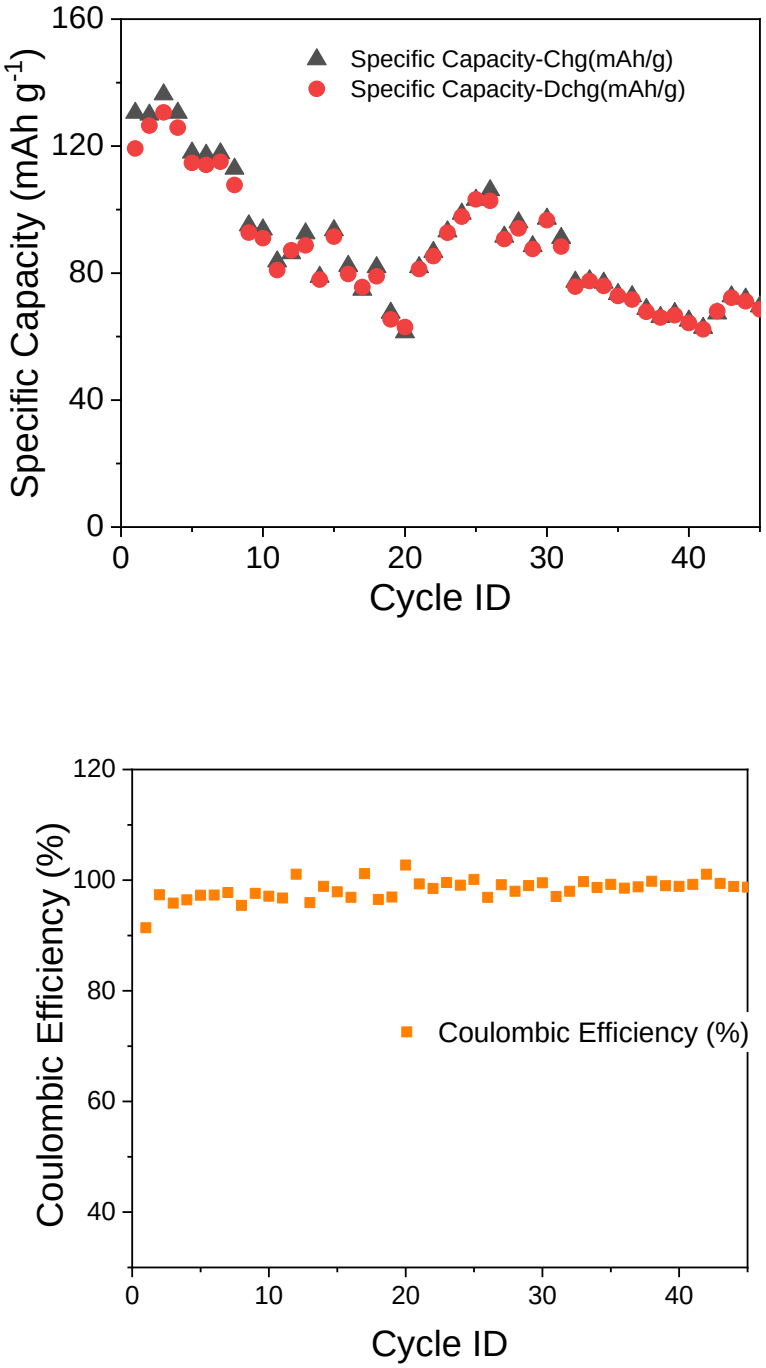

FIGURE 33 – Cycling Diagram of Solid-State Batteries Using Composite Electrolyte: (up) Discharge/Charge Specific Capacity; (down) Coulombic Efficiency.

V. CONCLUSIONS

In summary, we have gained deeper understanding on materials of hydrogenated carbon nanosheets and LPSCl-incorporated composite solid electrolyte membranes.

For hydrogenated carbon nanosheets that synthesized from solid-gas reactions, it is found that: (1) at 500 ˚C reaction, the H-content in the carbon nanosheets increases from 1.19% to 1.93% when the heating time decreases from 24 hours to 12 hours; (2) hydrogenated carbon nanosheets (500-12h and 500-24h) show broad D band and G band in Raman spectra; (3) the 500-24h sample exhibits higher electrical conductivity and lower sheet resistance (~45 Ohm/sq) than that of 500-12h sample (92 Ohm/sq); (4) hydrogenated carbon nanosheets can significant reduce the WVTR values on PET substrate and glass substrates by 50~60%. Higher hydrogen contents lead to lower WVTR values, indicating better pretension from water penetration.

For LPSCl-incorporated composite solid electrolyte, we have studied the compositions, and influence of synthetic parameters such as humidity and temperatures on the structure and conductivity. It was found that (1) for all compositions of composite solid electrolytes with LPSCl content from 10~30wt%, it is unstable to synthesis them in moderate humidity 40% RH and above, and there is no crystalline LPSCl remained in the composites; (2) it also cannot observed crystalline LPSCl when the composites were prepared under higher temperatures (40-70˚C) and higher humidity; (3) the ionic

conductivity is more sensitive to temperature instead of phase purity; (4) the assembled batteries showed maximum capacity being 138 mAh g^{-1} with a quick reduction to a stable 80-65 mAh g^{-1} show the potential of the electrolyte stability even after degradation of the material with the continued cycling suggesting reactions to take place prior to becoming a solid. Documentation about the physical features of the solid electrolyte is promising for providing a visual understanding of the reactions that take place in the membrane. Further research is required in order to provide consistent evidence towards a stable electrolyte in both the drying and finished product.

.

VI. RECOMMENDATIONS

The purpose of solid electrolytes is to form a safer and stable material that can perform with the ability to replace the liquid electrolyte business and stride towards a safer developed electric powered future. The use of polymer composite material provides protection from atmospheric conditions, with this thesis demonstrating the statement is true post-fabrication. Recommendations towards this research is to develop a better understanding of the reactions and how to prevent them in an open environment or a production system fit to protect the material while drying cost-effectively. Stride towards improvement could be a dry room system that could have the reduced humidity necessary for preserving the material as its being mixed and dried. Further study on the hybrid argyrodite is needed to see any further improvement on the conductivity and specific capacity capabilities in battery performance consistently and in depth.

With studies being done on PSCs showing promising increase in stability, the potential of using hydrophobic coating to protect the moisture sensitive composite membranes could improve on how we use sustainable energy systems. Research towards solid state batteries could involve the hydrophobic carbon coating potential to further stability, monitoring how it affects the performance in both the strength of the battery but also the stability over longer periods of time in the attempt to reduce moisture exposure.

REFERENCES

1. Ali, S. R., Faisal, M. M., Sanal, K. C., & Iqbal, M. W. (2021). Impact of carbon-based charge transporting layer on the performance of Perovskite Solar Cells. *Solar Energy*, *221*, 254–274. https://doi.org/10.1016/j.solener.2021.04.040

2. Ahn N, et al. "Carbon-Sandwiched Perovskite Solar Cell." *Journal of Materials Chemistry A*, vol. 6, no. 4, 2018, pp. 1382–1389., https://doi.org/10.1039/c7ta09174e.

3. Babu, V., Pineda, R. F., Ahmad, T., Alvarez, A. O., Castriotta, L. A., Cario, A. D., Fabregat-Santiago, F., & Wojciechowski, K. (2020). Improved stability of inverted and flexible perovskite solar cells with carbon electrode. https://doi.org/10.1021/acsaem.0c00702.s001

4. Bai, X., Duan, Y., Zhuang, W., Yang, R., & Wang, J. (2020). Research progress in Li-argyrodite-based solid-state electrolytes. *Journal of Materials Chemistry A*, *8*(48), 25663–25686. https://doi.org/10.1039/d0ta08472g

5. Bureau of Reclamation, L. C. R. W. T. (n.d.). *Hoover dam*. Hoover Dam | Bureau of Reclamation. Retrieved April 20, 2022, from https://www.usbr.gov/lc/hooverdam/faqs/powerfaq.html#:~:text=Hydropower%20at%20Hoover%20Dam%20Hoover%20Dam%20generates%2C%20on,it%20is%20still%20one%20of%20the%20country%27s%20largest.

6. Deiseroth, H.J., Kong, S.T., Eckert, H., et al.: Li6PS5X: a class of crystalline Li-rich solids with an unusually high Li+ mobility. Angew. Chem. Int. Ed. 47, 755–758 (2008). https://doi.org/10.1002/anie.200703900

7. Dirican, M., Yan, C., Zhu, P., & Zhang, X. (2018). *Composite Solid Electrolytes for All-Solid-State Lithium Batteries*, *136*, 27–46.

8. Dong, Q., Liu, F., Wong, M. K., Tam, H. W., Djurišić, A. B., Ng, A., Surya, C., Chan, W. K., & Ng, A. M. (2016). Encapsulation of perovskite solar cells for high humidity conditions. *ChemSusChem*, *9*(18), 2597–2603. https://doi.org/10.1002/cssc.201600868

9. Dou, Q., Whatley, T., Syed, T., Wei, W., & Wang, H. (2022). Carbon nanomaterials–polymer composites for perovskite solar cells: Preparation, properties and applications. *Journal of Materials Chemistry A*. https://doi.org/10.1039/d2ta02175g

10. Electricity from landfill gas. (n.d.). Retrieved April 20, 2022, from http://www.powerscorecard.org/tech_detail.cfm?resource_id=5#:~:text=Large%20municipal%20or%20industrial%20landfills%20produce%20gas%20that,methane%20and%2040%20percent%20carbon%20dioxide%20%28or%20%22CO2%22%29.

11. Fan, X., Ji, X., Han, F., Yue, J., Chen, J., Chen, L., Deng, T., Jiang, J., & Wang, C. (2018). Fluorinated solid electrolyte interphase enables highly reversible solid-state Li Metal Battery. *Science Advances*, *4*(12). https://doi.org/10.1126/sciadv.aau9245

12. Gao, Z., Sun, H., Fu, L., Ye, F., Zhang, Y., Luo, W., & Huang, Y. (2018). Promises, challenges, and recent progress of Inorganic Solid-state electrolytes for all-solid-state lithium batteries. *Advanced Materials*, *30*(17), 1705702. https://doi.org/10.1002/adma.201705702

13. Gil-González, E., Ye, L., Wang, Y., Shadike, Z., Xu, Z., Hu, E., & Li, X. (2022). Synergistic effects of chlorine substitution in sulfide electrolyte solid state batteries. *Energy Storage Materials*, *45*, 484–493. https://doi.org/10.1016/j.ensm.2021.12.008

14. H. Lee, P. Oh, J. Kim, H. Cha, S. Chae, S. Lee and J. Cho, Advances and prospects of sul□de all-solid-state lithium batteries via one-to-one comparison with conventional liquid lithium ion batteries, Adv. Mater., 2019, 31(29), 1900376.

15. H. M. Chen, C. Maohua and S. Adams, Stability and ionic mobility in argyrodite-related lithium-ion solid electrolytes, Phys. Chem. Chem. Phys., 2015, 17(25), 16494–16506.

16. Kraft, M. A., Culver, S. P., Calderon, M., Böcher, F., Krauskopf, T., Senyshyn, A., Dietrich, C., Zevalkink, A., Janek, J., & Zeier, W. G. (1970, January 1). *Influence of lattice polarizability on the ionic conductivity in the lithium superionic argyrodites Li6PS5X (X = cl, br, I).: Semantic scholar*. undefined. Retrieved April 20, 2022, from https://www.semanticscholar.org/paper/Influence-of-Lattice-Polarizability-on-the-Ionic-in-Kraft-Culver/b4c9ee1ad5dc187707c3a5a09e7a90dd4e82f2aa

17. Lau, J., DeBlock, R. H., Butts, D. M., Ashby, D. S., Choi, C. S., & Dunn, B. S. (2018). Sulfide solid electrolytes for lithium battery applications. *Advanced Energy Materials*, *8*(27), 1800933. https://doi.org/10.1002/aenm.201800933

18. Lu, P., Liu, L., Wang, S., Xu, J., Peng, J., Yan, W., Wang, Q., Li, H., Chen, L., & Wu, F. (2021). Superior all-solid-state batteries enabled by a gas-phase-

synthesized sulfide electrolyte with ultrahigh moisture stability and ionic conductivity. *Advanced Materials*, *33*(32), 2100921. https://doi.org/10.1002/adma.202100921

19. Mao, B., Chen, H., Jiang, L., Zhao, C., Sun, J., & Wang, Q. (2020). Refined study on lithium ion battery combustion in open space and a combustion chamber. *Process Safety and Environmental Protection*, *139*, 133–146. https://doi.org/10.1016/j.psep.2020.03.037

20. Mesquita, I., Andrade, L., & Mendes, A. (2020). Effect of relative humidity during the preparation of perovskite solar cells: Performance and stability. *Solar Energy*, *199*, 474–483. https://doi.org/10.1016/j.solener.2020.02.052

21. Muy, S., Bachman, J. C., Giordano, L., Chang, H.-H., Abernathy, D. L., Bansal, D., Delaire, O., Hori, S., Kanno, R., Maglia, F., Lupart, S., Lamp, P., & Shao-Horn, Y. (2018). Tuning mobility and stability of lithium ion conductors based on lattice dynamics. *Energy & Environmental Science*, *11*(4), 850–859. https://doi.org/10.1039/c7ee03364h

22. Otoyama, M., Sakuda, A., Tatsumisago, M., & Hayashi, A. (2020). Sulfide electrolyte suppressing side reactions in composite positive electrodes for all-solid-state lithium batteries. *ACS Applied Materials & Interfaces*. https://doi.org/10.1021/acsami.0c05050

23. Ritchie, H., Roser, M., & Rosado, P. (2020, November 28). *Electricity mix*. Our World in Data. Retrieved April 20, 2022, from https://ourworldindata.org/electricity-mix#:~:text=Some%20countries%20get%20over%2090%25%20of%20their%20electricity,source%20%E2%80%93%20for%20countries%20in%20our%20work%20here.

24. Ruhl, J., Riegger, L. M., Ghidiu, M., & Zeier, W. G. (2021). Impact of solvent treatment of the superionic argyrodite Li 6 ps 5 cl on solid-state battery performance. *Advanced Energy and Sustainability Research*, *2*(2), 2000077. https://doi.org/10.1002/aesr.202000077

25. Simon, F. J., Hanauer, M., Richter, F. H., & Janek, J. (2020). Interphase Formation of PEO20:litfsi–li6ps5cl composite electrolytes with Lithium Metal. *ACS Applied Materials & Interfaces*, *12*(10), 11713–11723. https://doi.org/10.1021/acsami.9b22968

26. Stable and Flexible Sulfide Composite Electrolyte for High-Performance Solid-State Lithium Batteries ACS Applied Materials and Interfaces 12(38):42653-42659 American Chemical Society 2020 1944-8244

27. Sustainabilityinfo. (2022, February 16). *Sustainabilityinfo*. Sustainability Info. Retrieved April 20, 2022, from https://sustainabilityinfo.com/energy/how-much-

electricity-do-wind-turbines-generate/#:~:text=Wind%20turbines%20generate%20electricity%20by%20capturing%20the%20kinetic,A%20wind%20turbine%20generates%20about%201.64%20megawatts%20%28MW%29.

28. Taklu, B. W., Su, W.-N., Nikodimos, Y., Lakshmanan, K., Temesgen, N. T., Lin, P.-X., Jiang, S.-K., Huang, C.-J., Wang, D.-Y., Sheu, H.-S., Wu, S.-H., & Hwang, B. J. (2021). Dual CuCl doped argyrodite superconductor to boost the interfacial compatibility and air stability for all solid-state lithium metal batteries. *Nano Energy*, *90*, 106542. https://doi.org/10.1016/j.nanoen.2021.106542

29. Tiep, N. H., Ku, Z., & Fan, H. J. (2015). Recent advances in improving the stability of perovskite solar cells. *Advanced Energy Materials*, *6*(3), 1501420. https://doi.org/10.1002/aenm.201501420

30. Yao, X., Huang, B., Yin, J., Peng, G., Huang, Z., Gao, C., Liu, D., & Xu, X. (2016). All-solid-state lithium batteries with inorganic solid electrolytes: Review of fundamental science. *Chinese Physics B*, *25*(1), 018802. https://doi.org/10.1088/1674-1056/25/1/018802

31. Yu, C., Zhao, F., Luo, J., Zhang, L., & Sun, X. (2021). Recent development of lithium argyrodite solid-state electrolytes for solid-state batteries: Synthesis, structure, stability and Dynamics. *Nano Energy*, *83*, 105858. https://doi.org/10.1016/j.nanoen.2021.105858

32. Zhao, W., Yi, J., He, P., & Zhou, H. (2019). Solid-state electrolytes for lithium-ion batteries: Fundamentals, challenges and Perspectives. *Electrochemical Energy Reviews*, *2*(4), 574–605. https://doi.org/10.1007/s41918-019-00048-0

33. Ziolkowska, D. A., Arnold, W., Druffel, T., Sunkara, M., & Wang, H. (2019). Rapid and economic synthesis of a li7ps6 solid electrolyte from a liquid approach. *ACS Applied Materials & Interfaces*, *11*(6), 6015–6021. https://doi.org/10.1021/acsami.8b19181

34. Z. Zhang, Y. Sun, X. Duan, L. Peng, H. Jia, Y. Zhang, B. Shan and J. Xie, Design and synthesis of room temperature stable Li-argyrodite superionic conductors via cation doping, J. Mater. Chem. A, 2019, 7(6), 2717–2722

APPENDIX

NOMENCLATURE

A, is the surface area (cm)

t, is the thickness (cm)

Ω, is the level of resistance (ohm)

σ, is the ionic conductivity (S cm^{-1})

I, is the current (mA)

m_T, is the total mass weighed (mg)

CURRICULUM VITA

NAME: Tanner Davis Whatley

ADDRESS: Conn Center for Renewable Energy Research
2929 S Floyd St
University of Louisville
Louisville, KY 40209

DOB: Louisville, KY – June 26th, 1999

EDUCATION & TRAINING:

B. S. Mechanical Engineering
Western Kentucky University
2017-20

M. S. Mechanical Engineering
University of Louisville
2021-22

Graduate Research Assistant
University of Louisville
2021-22

AWARDS: Dean's List of Engineering Department
Western Kentucky University
2020

PUBLICATIONS: Dou, Q., Whatley, T., Syed, T., Wei, W., & Wang, H. (2022). Carbon nanomaterials–polymer composites for perovskite solar cells: Preparation, properties and applications. *Journal of Materials Chemistry A*. https://doi.org/10.1039/d2ta02175g